Acta Pharmaceutica Sinica B 2018;8(6):889–899

Chinese Pharmaceutical Association
Institute of Materia Medica, Chinese Academy of Medical Sciences

Acta Pharmaceutica Sinica B

www.elsevier.com/locate/apsb
www.sciencedirect.com

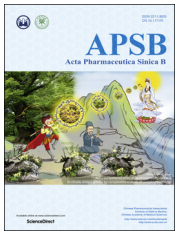

ORIGINAL ARTICLE

High-throughput screening for small molecule inhibitors of the type-I interferon signaling pathway

Elita Yuliantie[a,b], Xinchuan Dai[a], Dehua Yang[a,b], Peter J. Crack[c], Ming-Wei Wang[a,b,d,*]

[a]*The National Center for Drug Screening and the CAS Key Laboratory of Receptor Research, Shanghai Institute of Materia Medica, Chinese Academy of Sciences (CAS), Shanghai 201203, China*
[b]*University of Chinese Academy of Sciences, Beijing 100049, China*
[c]*Department of Pharmacology and Therapeutics, The University of Melbourne, Parkville, Victoria 3010, Australia*
[d]*School of Pharmacy, Fudan University, Shanghai 201203, China*

Received 28 March 2018; received in revised form 26 May 2018; accepted 21 June 2018

KEY WORDS

High-throughput screening;
Interferon α receptor;
Secreted embryonic alkaline phosphatase;
JAK-STAT;
IFN regulatory factor;
Inhibitor

Abstract Interferons (IFNs) are cytokines with fundamental roles in resistance to infections, cancer and other diseases. Type-I IFNs, interferon α (IFN-α) and interferon β (IFN-β), act through a shared receptor complex (IFNAR) comprised of IFNAR1 and IFNAR2 subunits. Binding of type-I IFN to IFNAR1 will robustly activate Janus activated kinase-signal transducer and activator of transcription (JAK-STAT) signaling pathway. Aberrant activation of the type-I IFN response results in a spectrum of disorders called interferonopathies. The purpose of this research is to develop an assay for high-throughput screening (HTS) of small molecule inhibitors of the type-I IFN signaling pathway. Inhibition of type-I IFN signaling can be beneficial in terms of therapeutic use and understanding the underlying mechanism of action. We report here a HTS campaign with the secreted embryonic alkaline phosphatase (SEAP) reporter gene assay against 32,000 compounds which yielded 25 confirmed hits. These compounds were subsequently characterized for their cytotoxicity, effects on STAT phosphorylation and activities in IFN regulatory factor (IRF) transcription.

Abbreviations: cDNA, complementary DNA; CV, coefficient of variation; DMEM, Dulbecco's modified Eagle's medium; DMSO, dimethyl sulfoxide; FRET, fluorescence resonance energy transfer; HEK, human embryonic kidney; HTS, high-throughput screening; IFN, interferon; IFNAR, IFN alpha receptor; IRF, IFN regulatory factor; ISGF3, IFN-stimulated gene factor 3; ISRE, IFN-stimulated response element; JAK, Janus activated kinase; pSTAT, phosphorylated STAT; *S/B*, signal to background ratio; SEAP, secreted embryonic alkaline phosphatase; STAT, signal transducer and activator of transcription; TYK, tyrosine kinase

*Corresponding author at: The National Center for Drug Screening and the CAS Key Laboratory of Receptor Research, Shanghai Institute of Materia Medica, Chinese Academy of Sciences (CAS), Shanghai 201203, China.
E-mail address: mwwang@simm.ac.cn (Ming-Wei Wang).

Peer review under responsibility of Institute of Materia Medica, Chinese Academy of Medical Sciences and Chinese Pharmaceutical Association.

https://doi.org/10.1016/j.apsb.2018.07.005

1. Introduction

Interferons (IFN) are pleiotropic cytokines involved in innate and adaptive immunity. Classified into types I, II and III, they play fundamental roles in resistance to infections, cancer, and other diseases[1]. Type-I IFNs comprise 14 IFN-αs, IFN-β, IFN-ε, and IFN-ω[2]. IFN-α and IFN-β are both used for treatment of a wide range of diseases: IFN-α2a for chronic hepatitis C, IFN-α2b for malignancies, and IFN-β1a for multiple sclerosis[3,4]. Their side-effects include neurological and hematologic toxicities[5]. Aberrant activation of type-I IFN response results in a spectrum of disorders called interferonopathies, such as Aicardi-Goutieres syndrome, chronic autoinflammatory systemic lupus erythematosus, and cerebrovascular disease[6–8].

Type-I IFN response occurs when IFN-α/β binds to their receptor complex, IFNAR. This receptor complex is comprised of two subunits: IFNAR1 and IFNAR2. The ligand–receptor complex is phosphorylated, presumably by pre-associated Janus activated kinases (JAKs) namely tyrosine kinase 2 (TYK2) on IFNAR1 and JAK1 on IFNAR2. The phosphorylated receptors are docking sites for signal transducers and activators of transcription (STAT) factors that dimerise and translocate to the nucleus. STATs 1, 2, 3, 4, and 5 are activated by type-I IFNs in many cell types. Other kinases (*e.g.*, mitogen-activated protein kinases) and transcription factors (*e.g.*, nuclear factor-κB) can also be activated in response to type-I IFNs. Multiple pathways and IFN-regulated genes are activated by IFNs, many of which remain unknown[9].

Clearly, inhibition of IFN signaling can be beneficial in terms of therapeutic use and understanding the underlying molecular and cellular mechanisms. Several attempts have been tried to develop JAK or STAT inhibitors as well as monoclonal antibodies against IFN-α and IFN receptor antagonists[10,11]. For instance, AstraZeneca-Medimmune developed anifrolumab (formerly known as MEDI-546), a fully human immunoglobulin G1κ monoclonal antibody directed against IFNAR1 for treatment of systemic lupus erythematosus which is currently undergoing phase 3 clinical trials[12].

High-throughput screening (HTS) efforts in identifying JAK and STAT inhibitors have been made[13–16]. Nonetheless, up to now there is only one reported small molecule inhibitor with clinical efficacy for this pathway[17]. Here we describe an HTS assay capable of discovering potential inhibitors of type-I IFN signaling. HTS was applied to screen 32,000 compounds which resulted in 25 confirmed hits. This was followed by characterization for compound cytotoxicity in stably engineered human embryonic kidney (HEK) and neuroblastoma SH-SY5Y cells. As type-I IFN is implicated in neuronal inflammation[18,19], SH-SY5Y cell line was thus chosen as a potential model for testing bioactivities. This cell line has also been shown to possess an active JAK-STAT signaling and the ability to provoke inflammatory reaction upon type-I IFN treatment[20,21]. Functional effects of the hits on JAK-STAT signaling, including STAT phosphorylation and IFN regulatory factor (IRF) mRNA expression were studied in parallel.

2. Materials and methods

2.1. Compounds

The chemical compound library used for the screening of type-I interferon signaling pathway inhibitors consisted of 32,000 synthetic and natural products derived pure compounds. All the compounds come from the Chinese National Compound Library (www.cncl.org.cn). The structural diversity covers heterocycles, lactams, sulfonates, sulfonamides, amines and secondary amides. Compounds with the code of WNN are proprietary in our collection and the others are commercially available. They are stored at concentrations of 5 mg/mL and 1 mg/mL in 100% dimethyl sulfoxide (DMSO), respectively. Compounds were diluted in cell medium for each assay.

2.2. Chemicals and antibodies

Niclosamide (Selleck Chemicals, Houston, TX, USA) was initially diluted in 33% dimethylacetylamine and 67% PEG400 to 25 mmol/L stock concentration. Cells were treated with test compounds at a concentration of 10 μmol/L. Recombinant human IFN-α2a (Novoprotein, Shanghai, China) is produced by *Escherichia coli* expressing Cys24-Glu188. Interferon was dissolved in distilled water, aliquoted, and stored at a concentration of 2×10^4 IU/mL. Antibodies used were STAT1 (D1K9Y), Phospho-STAT1 (Tyr701) (58D6), STAT3 (79D7), Phospho-STAT3 (Tyr705) (D3A7) XP®, and β-actin made in rabbits; goat anti-rabbit IgG HRP-linked antibody (Cell Signaling Technology, Danvers, MA, USA), and GAPDH mouse mAb 39–8600 (ZG003) (ThermoFisher Scientific, Waltham, MA, USA), and goat anti-mouse IgG-HRP (Santa Cruz Biotechnology, Santa Cruz, CA, USA). The assay plates (SpectraPlate™-384 TC) were produced by PerkinElmer (Boston, MA, USA).

2.3. Cell lines

HEK-Blue IFNα/β cells, QUANTI-Blue, zeocin, and blasticidin were purchased from Invivogen (Carlsbad, CA, USA). HEK-Blue IFNα/β cells are specifically designed to monitor the activation of the JAK-STAT pathway induced by type-I IFNs. This cell line was maintained in Dulbecco's modified Eagle's medium (DMEM) with 10% fetal bovine serum, 30 μg/mL of blasticidin and 100 μg/mL of zeocin in a 37 °C, 5% CO_2 incubator. Human neuroblastoma cells, SH-SY5Y, were cultured in DMEM with 10% fetal bovine serum, 50 U/mL penicillin and 50 μg/mL streptomycin. DMEM, fetal bovine serum, 0.25% Trypsin-EDTA were bought from Life Technologies (Carlsbad, CA, USA). DMSO was procured from Sigma (St Louis, MO, USA).

2.4. Treatment

HEK-Blue IFNα/β and SH-SY5Y cells were treated with IFN-α2a at concentrations of 150 IU/mL for 15 min and 300 IU/mL for

30 min, respectively. Compounds were added 15 min before IFN treatment in fresh culture medium for protein and RNA isolation.

2.5. High-throughput screening

Compounds (0.5 μL/well) were dissolved in DMSO and added into 384-well plates prior to seeding HEK-Blue IFNα/β (5,000/well). The mixture was kept in a 37 °C, 5% CO_2 incubator for 5 h. IFN-α2a was then added to the plates to make final concentration of 150 IU/mL. The wells were incubated at 37 °C, 5% CO_2 overnight. Seven microliters supernatant of each well was transferred to the new assay plate followed by addition of QUANTI-Blue (72 μL/well). The wells were incubated for 2 h at 37 °C. The absorbance of 640 nm was read by FlexStation^{III} (Molecular Device, Sunnyvale, CA, USA).

Samples dissolved in 100% DMSO were applied to the primary screening, with an average final concentration of 20 μmol/L for each compound. In each 384-well assay plate, 24 wells were used as positive control (1% DMSO with 10 μmol/L niclosamide and 150 IU/mL IFN-α2a), 24 wells as negative control (1% DMSO with 150 IU/mL IFN-α2a without any compounds), and 16 wells as blank control (1% DMSO without IFN-α2a and compounds). Compounds showing greater than 70% inhibition relative to negative controls were considered "hits".

2.6. Dose response

Dose–response study was performed essentially as the same as described above except that test compounds were hand-picked (average stock concentration: 10 mmol/L) and diluted (1:5) seven times to give a total of eight serial diluents. The final compound concentration was ranging from 100 μmol/L to 1.28 nmol/L. Each compound was tested in triplicate.

2.7. Data analysis

Z' factor was evaluated in 48 positive control wells, 48 negative control wells and 32 blank control wells before the HTS campaign as following:

$$Z' = 1 - \frac{3 \times (\mathrm{SDPC} + \mathrm{SDNC})}{|\mathrm{MPC} - \mathrm{MNC}|} \quad (1)$$

where MPC means the mean value of positive control wells; SDPC means the standard deviation of positive control wells; MNC means the mean value of negative control wells; and SDNC means the standard deviation of negative control wells.

The equation of inhibition (%) is as following:

$$\text{Inhibition } (\%) = \left(1 - \frac{\mathrm{Signal}_{\mathrm{test}} - \mathrm{Signal}_{\mathrm{blank}}}{\mathrm{Signal}_{\mathrm{NC}} - \mathrm{Signal}_{\mathrm{blank}}}\right) \times 100 \quad (2)$$

where $\mathrm{Signal}_{\mathrm{test}}$ means the value of each compound test well; $\mathrm{Signal}_{\mathrm{blank}}$ means the mean value of blank control wells; and $\mathrm{Signal}_{\mathrm{NC}}$ means the mean value of negative control wells.

2.8. Cytotoxicity assay

Cells were cultured in 96-well plate until 60%–80% density was reached. Compounds were prepared to give five different final concentrations: 50, 25, 12.5, 6.25, and 3.125 μmol/L. Non-treated control and blank (medium only) control were placed in each plate. Twenty-four hour compound incubation was followed by addition of CCK8 solution (Dojindo, Kumamoto, Japan) to each well. Absorbance at 450 nm 3 h thereafter was measured by an Envision plate reader (PerkinElmer). Cell viability (%) was calculated compared to the non-treated and blank wells.

Table 1 Primer pairs used for quantitative PCR (pga.mgh.harvard.edu).

Gene	Position	Primer sequence
IRF3	Forward	AGAGGCTCGTGAATGGTCAAG
	Reverse	AGGTCCACAGTATTCTCCAGG
IRF7	Forward	GCTGGACGTGACCATCATGTA
	Reverse	GGGCCGTATAGGAACGTGC
GAPDH	Forward	GAAGGTGAAGGTCGGAGT
	Reverse	GAAGATGGTGATGGGATTTC

2.9. Protein extraction and western blot analysis

HEK-Blue IFNα/β and SH-SY5Y cells were grown for 48 h until reach confluence in 24-well plates. 5 × SDS-PAGE loading buffer stock and 8% SDS-PAGE gel were prepared according to standard protocol. The material used were Tris base, tetramethylethylenediamine, ammonium persulfate (Sigma), SDS (OurChem, Guangdong, China), bromphenol blue, glycerol, hydrochloric acid (SCR, Shanghai, China), β-mercaptoethanol (Fluka Chemie, Buchs, Switzerland) and 30% acrylamide (Generay Biotech, Shanghai, China).

Protein was extracted by 1 × SDS-PAGE loading buffer, 100 μL per well. Cells were scraped from the plate and put into chilled tube. Denaturation was carried out by boiling at 100 °C for 10 min. Protein extract was loaded into 1 mm thick gel, each well was given 45 μg, and run for stacking 30 V for 30 min and then 120 V for 1 h with 1 × SDS running buffer (10 × recipe is 30.2 g Tris-base, 188 g glycine from SCR, 10 g SDS, and distilled water to make 1 L). Protein was then transferred to Immobilon-P PVDF membrane (Merck, Darmstadt, Germany) for 1 h at 100 V on ice by wet transfer. Rapid Transfer Buffer (EpiZyme Biotech, Shanghai, China) was used with addition of 15% methanol. Membrane was blocked by 5% skim milk in TBST (EpiZyme Biotech) for 1 h. Primary antibodies were diluted according to the manual, incubated with membrane for 16 h at 4 °C. Membrane was washed three times in TBST. Incubation with secondary antibodies was for 1 h at room temperature. Signal was enhanced by Super Signal® West Dura Extended Duration Substrate (ThermoFisher Scientific). Images were analyzed with ImageJ software (National Institutes of Health, Bethesda, MA, USA). Percent inhibition of compound was calculated compared to non-treated controls (100% inhibition) and IFN treatment (no inhibition).

2.10. RNA isolation and quantitative PCR

Total RNA from confluent monolayer cells in 12-well plate was isolated with 500 μL/well TRIzol reagent (Ambion, Carlsbad, CA,

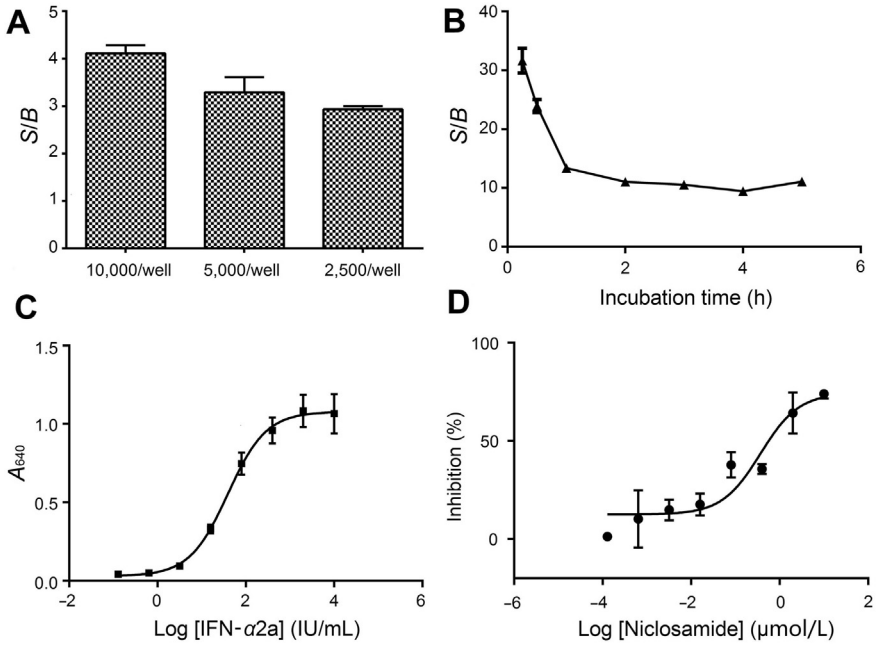

Figure 1 Optimization for the HTS assay. (A) Signals after treatment with IFN-α2a (200 IU/mL) with different number of cells were measured ($n=3$). (B) Activities of different incubation time with QUANTI-Blue (0–5 h) after treatment with IFN-α2a (200 IU/mL) were measured ($n=3$). (C) IFN-α2a titration (0.128 to 10,000 IU/mL, $n=3$). (D) Dose-response curve of niclosamide upon IFN-α2a treatment measured with the optimal assay conditions, from which IC_{50} value was calculated ($n=3$).

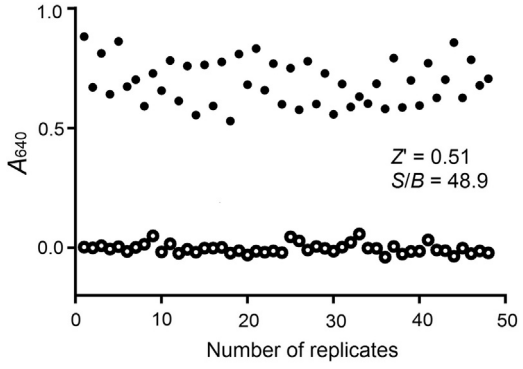

Figure 2 Z' factor of the HTS assay was determined under the optimized conditions. Forty-eight replicates of signal (negative control, black circle) and background (positive control, white circles) were investigated.

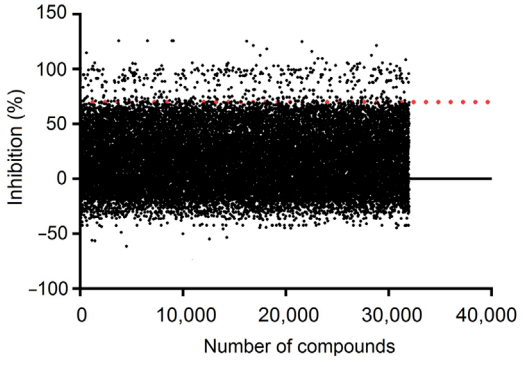

Figure 3 HTS campaign of 32,000 compounds using SEAP reporter assay. The results are expressed as percentage of inhibition of each sample on SEAP response induced by IFN-α2a. Dashed line shows the cut off at 70% inhibitory activity. 457 hits (1.4%) showed higher than 70% inhibition in the primary screening.

USA) and the concentration measured by Nanodrop. Two μg of RNA was reverse transcribed into complementary DNA (cDNA) using the High Capacity cDNA Reverse Transcription Kit (Applied Biosystems, Foster City, CA, USA). Primer pairs (Table 1) were ordered from Genewiz (Jiangsu, China). Quantitative PCR was performed with 100 ng cDNA using SYBR Select Master Mix (Applied Biosystems). Each sample was done in triplicate and repeated three times. Relative expression of the gene of interest was calculated by the delta-delta Ct method with GAPDH as endogenous control.

2.11. *Statistical analysis*

Dose–response curves and IC_{50} values were generated using log (inhibitor) *vs.* response equation in nonlinear regression analysis. Data are expressed as means ± SEM. The significance was evaluated by a one-way analysis of variance (ANOVA) followed by Bonferroni *post hoc* test. Differences were considered significant when a P value was less than 0.05. All statistical analyses were performed with GraphPad Prism software version 5 (San Diego, CA, USA).

3. Results

3.1. *Assay validation*

Different numbers of cells (2500/well, 5000/well and 10,000/well) were employed to assess the optimal number of cells for the screening assay. The number of cells for each well was determined

Table 2 Structures of 25 confirmed hits and their IC_{50} values.

Compd.	Structure	Chemical formula	MW	IC_{50} (μmol/L)
WNN2202-B006	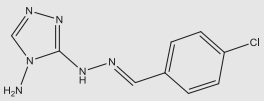	$C_9H_9ClN_6$	236.661	10.48
WNN2210-B007	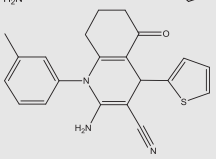	$C_{21}H_{19}N_3OS$	361.46	NA
WNN2210-C004	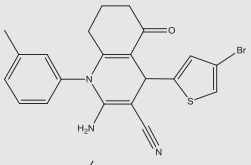	$C_{21}H_{18}BrN_3OS$	440.356	13.94
WNN2290-B006	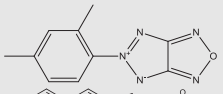	$C_{10}H_9N_5O$	215.211	6.522
CD2001-B009	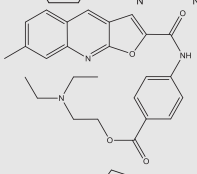	$C_{26}H_{27}N_3O_4$	445.51	15.69
CD2006-A002	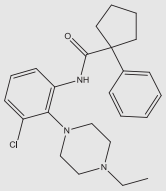	$C_{24}H_{30}ClN_3O$	411.967	3.39
CD2015-G003	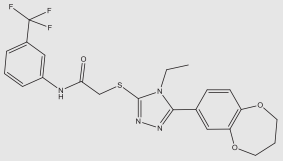	$C_{22}H_{21}F_3N_4O_3S$	478.487	5.478
CD2020-G009	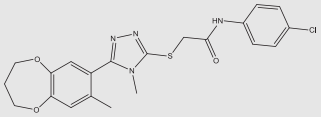	$C_{21}H_{21}ClN_4O_3S$	444.934	3.195
CD2047-G004	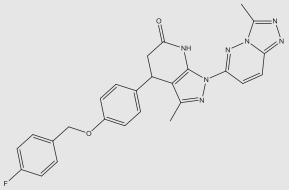	$C_{26}H_{22}FN_7O_2$	483.497	20.29
CD2079-E003	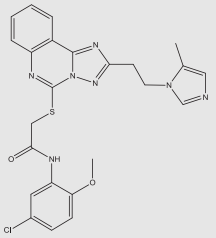	$C_{24}H_{22}ClN_7O_2S$	507.995	2.993
CD2093-G007	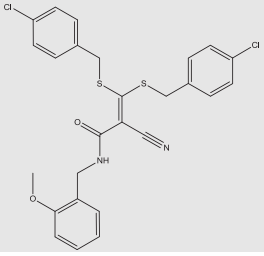	$C_{26}H_{22}Cl_2N_2O_2S_2$	529.501	0.2976

Table 2 (*continued*)

Compd.	Structure	Chemical formula	MW	IC_{50} (μmol/L)
CD2100-B008	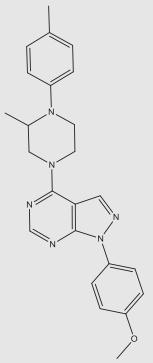	$C_{24}H_{26}N_6O$	414.503	43.34
JK3038-D010	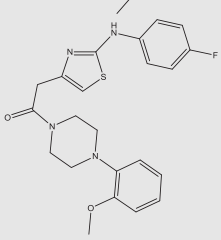	$C_{22}H_{23}FN_4O_2S$	426.507	2.959
JK3043-F003	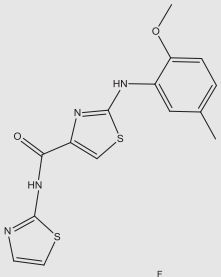	$C_{15}H_{14}N_4O_2S_2$	346.427	5.88
JK3049-H002	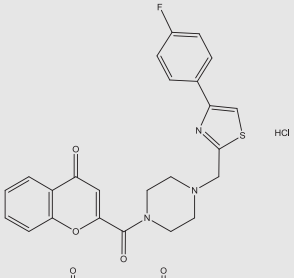	$C_{24}H_{21}ClFN_3O_3S$	485.958	3.777
JK3051-A002	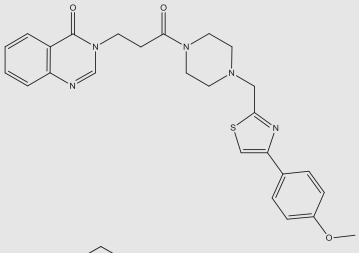	$C_{26}H_{27}N_5O_3S$	489.589	4.194
JK3090-H004	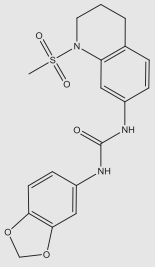	$C_{18}H_{19}N_3O_5S$	389.426	3.316

Table 2 (*continued*)

Compd.	Structure	Chemical formula	MW	IC_{50} (μmol/L)
RUS0903-C006	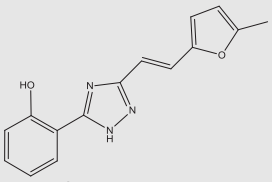	$C_{15}H_{13}N_3O_2$	267.283	1.492
RUS0910-G009	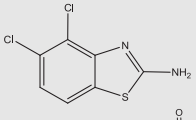	$C_7H_4Cl_2N_2S$	219.091	3.144
RUS0937-A002	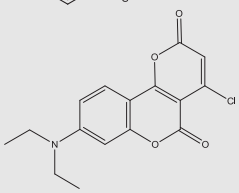	$C_{16}H_{14}ClNO_4$	319.74	2.263
RUS0948-D009	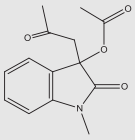	$C_{14}H_{15}NO_4$	261.273	4.984
RUS0966-F006		$C_{18}H_{17}N_3O_3S_3$	419.541	7.88
RUS0971-B008	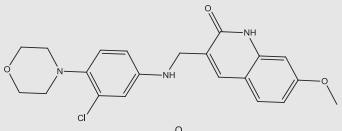	$C_{21}H_{22}ClN_3O_3$	399.871	4.917
RUS0971-C008	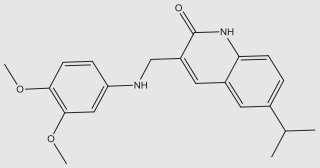	$C_{21}H_{24}N_2O_3$	352.427	20.91
RUS0998-A003	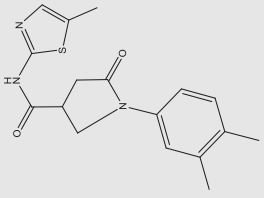	$C_{17}H_{19}N_3O_2S$	329.417	4.883

NA, not active.

to be 5000 (Fig. 1A). The result of incubation time evaluation of QUANTI-Blue course was shown in Fig. 1B. QUANTI-Blue is a solution which in the presence of any alkaline phosphatase changes color from pink to purple-blue. In combination with the secreted reporter, embryonic alkaline phosphatase (SEAP), it offers many advantages over intracellular reporters. Since the signal/background (*S*/*B*) ratio did not change significantly between 1 and 5 h, 2 h was selected. IFN-α2a titration was performed to choose the optimal concentration (Fig. 1C) and EC_{80} (150 IU/mL) was chosen for the assay. EC_{80} depicts the concentration which elicited 80% of the IFN-α2a response and signal represents the value of cells treated with IFN-α2a compared to blank control. Under these optimized conditions, the IC_{50} value of the positive molecule niclosamide was 0.37 μmol/L (Fig. 1D). It is in agreement with a previous study in which niclosamide dose-dependently inhibited STAT3 mediated luciferase reporter activity with an IC_{50} of 0.25 μmol/L in HeLa cells after 24 h incubation[22].

3.2. *Assay performance*

Both signals evoked by negative control (IFN-α2a stimulation) and by positive control (background) were studied. As shown in Fig. 2, the coefficient of variation (CV) value was 13.3% for

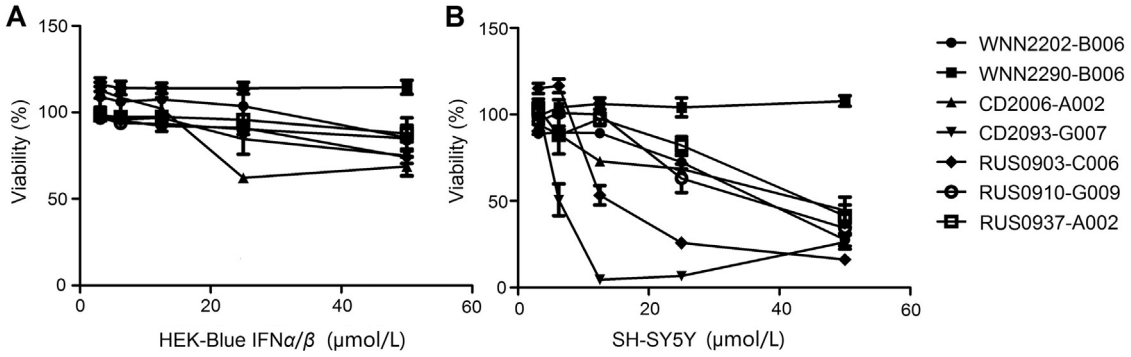

Figure 4 Viability of HEK-Blue IFNα/β (A) and SH-SY5Y (B) cells after 24 h incubation with hit compounds at 50, 25, 12.5, 6.25, and 3.125 μmol/L. Viability (%) was calculated compared to the non-treated control (100% viable) and blank (0% viable).

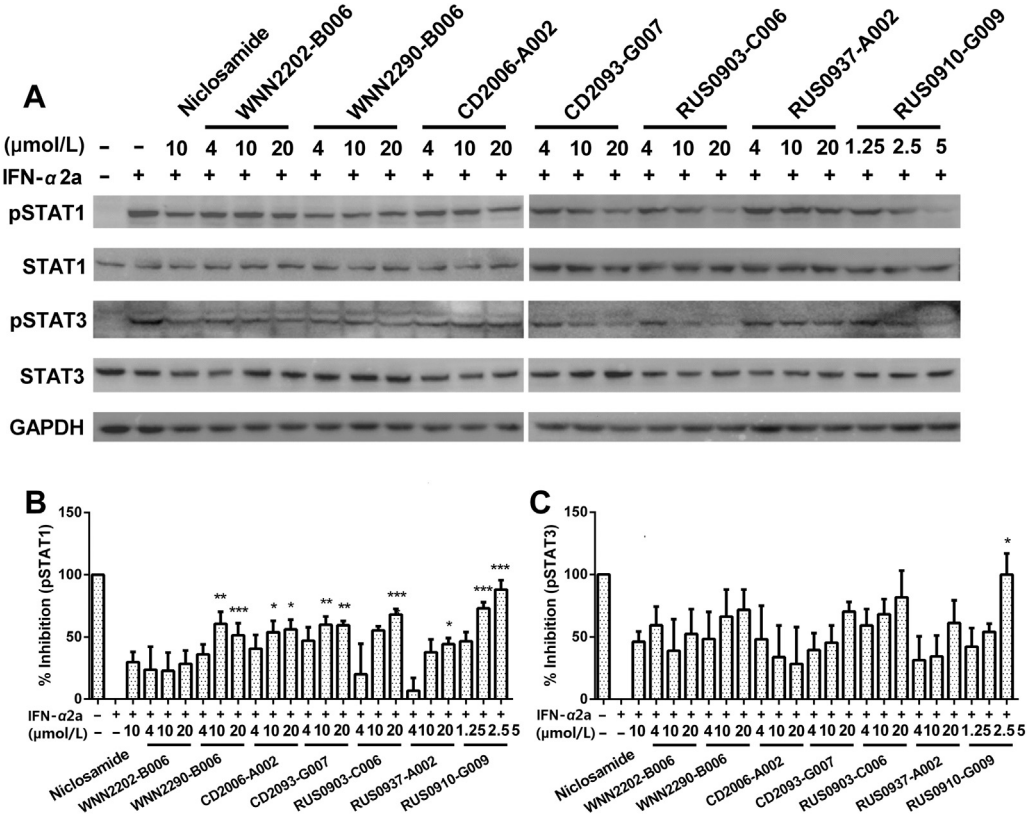

Figure 5 Some confirmed hits reduced STAT phosphorylation in response to IFN-α2a treatment (150 IU/mL, 15 min) in HEK-Blue IFNα/β cells. (A) Representative western blots of 7 hits in three different concentrations. (B) and (C) Inhibition (%) of pSTAT1 and pSTAT3 after treatment. Protein levels were determined by western blotting and normalized to GAPDH. Two SDS gels were used for each experiment. Data represent means ± SEM from at least three independent experiments. $^{*}P<0.05$, $^{**}P<0.01$, $^{***}P<0.001$ compared to IFN-α2a treated cells.

signal of IFN-α2a stimulation and the Z' factor was 0.51 with an S/B ratio of 48.9. These characteristics indicate that the system is of high quality and well-suited to HTS[23].

3.3. *Identification of inhibitors of type-I interferon signaling pathway*

Results of the primary screening of type-I interferon signaling pathway against 32,000 compounds are shown in Fig. 3. 457 hits (1.4%) that displayed inhibitory activity higher than 70% were picked for confirmation. In the secondary screening (initial hits in duplicates), 25 compounds demonstrated consistent inhibition and dose-dependency at the two concentration studied (20 and 4 μmol/L; Table 2 and Supplementary Information Fig. S1).

3.4. *Preliminary characterization of confirmed hits*

Twenty-five confirmed hits were assessed for their effects on phosphorylation of STAT1 and STAT3 (Supplementary Information Fig. S2). Of which, 7 compounds significantly

reduced the phosphorylation level of STAT1 and/or STAT3 at 20 μmol/L. WNN2202-B006, WNN2290-B006, CD2093-G007 and CD2006-A002 distinctly inhibited pSTAT3, while RUS0903-C006, RUS0910-G009 and RUS0937-A002 suppressed pSTAT1.

3.5. *Cytotoxicity measurement*

The above 7 confirmed hits were evaluated for cytotoxicity using the CCK8 assay kit. Treatment of SH-SY5Y cells with IFN-α2a up to 800 IU/mL did not affect cell viability (Data not shown). Among the seven, WNN2290-B006 showed no toxicity for both cell lines (Fig. 4). RUS0910-G009 and RUS0937-A002 were slightly toxic at the highest concentration in HEK cells while the rest demonstrated certain degree of toxicity. Neuroblastoma cell line SH-SY5Y was more sensitive towards the compounds. Six reduced cell viability by 50% or more at the highest concentration tested (50 μmol/L), whereas at 25 μmol/L only two hits (CD2093-G007 and RUS0903-C006) decreased viability to less than 50%.

3.6. *Effect on STAT1/STAT3 phosphorylation*

Binding of type-I IFN to IFNAR will activate STAT1 and STAT2. In addition, STAT3 and STAT5 are also known to be phosphorylated. STAT1 induces pro-inflammatory genes and inhibits cell growth while STAT3 homodimers indirectly suppress pro-inflammatory gene expression and stimulate growth[24]. Consistent with the literature[21,25], IFN-α2a induced robust phosphorylation of STAT1 and STAT3 in both cell lines as shown in Fig. S2, Figs. 5 and 6. Niclosamide was previously reported to only inhibit STAT3 phosphorylation at concentrations below 10 μmol/L[22]. Interestingly, in this study, a relatively high concentration (10 μmol/L) of niclosamide also inhibited STAT1 phosphorylation (Figs. 5B, 6B and Fig. S2).

Seven hits were studied in three concentrations (20, 10 and 4 μmol/L) with HEK-Blue IFNα/β cells (Fig. 5). Four compounds (CD2006-A002, RUS0903-C006, RUS0937-A002 and RUS0910-G009) showed dose-dependent suppression on STAT1 and five compounds (WNN2290-B006, CD2093-G006, RUS0903-C006, RUS0937-A002 and RUS0910-G009) inhibited STAT3 phosphorylation. Of the seven, five relatively non-toxic hits were tested in three concentrations (20, 10 and 4 μmol/L) on SH-SY5Y cells (Fig. 6): they dose-dependently suppressed STAT1 and STAT3 phosphorylation at various potencies. Compound RUS0910-G009 showed the highest potency among them.

3.7. *Effect on IRF7 mRNA transcription*

IRF3 and IRF7 are essential IRFs required to induce *IFN-α/β* gene transcription. Moreover, IRF7 is markedly elevated in all cell types by type-I IFN[26]. In most cases, transcription of these regulatory factors is triggered by STAT1/STAT2/IRF9 heterodimeric complex, namely, IFN-stimulated gene factor 3 (ISGF3), through an IFN-stimulated response element (ISRE) binding site[1,27].

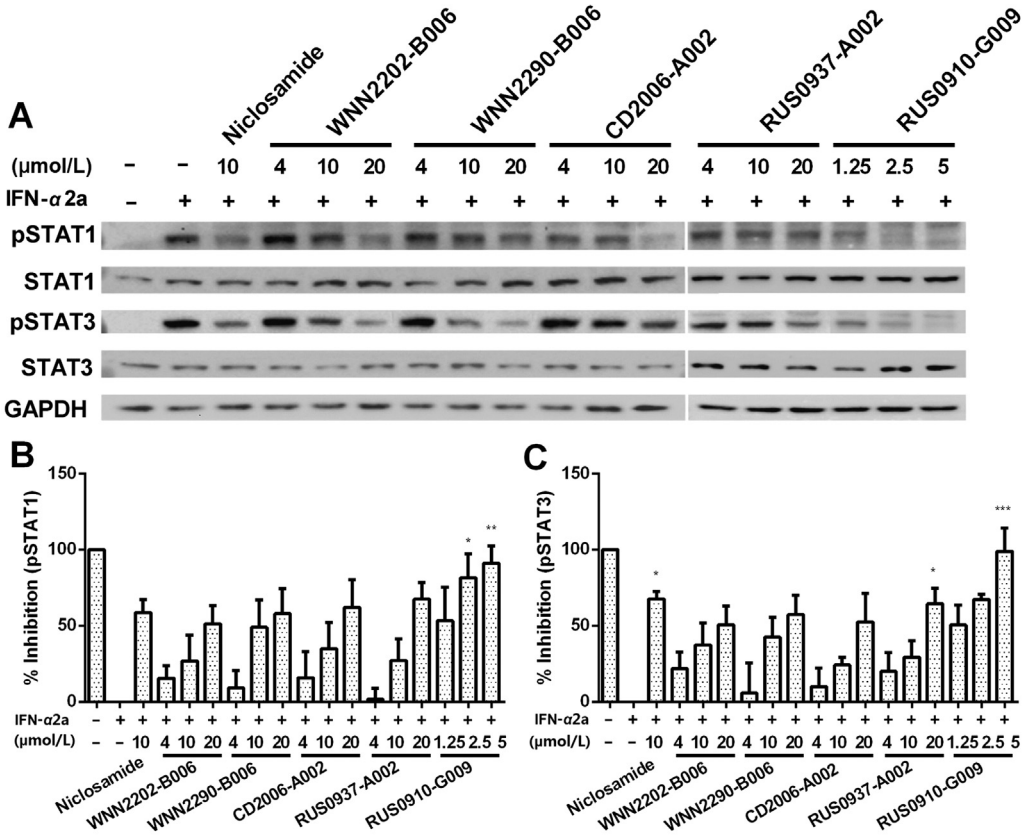

Figure 6 Some confirmed hits reduced STAT phosphorylation in response to IFN-α2a treatment (300 IU/mL 30 min) in SH-SY5Y cells. Representative western blots (A), inhibition (%) of pSTAT1 (B) and pSTAT3 (C) after treatment are shown. Protein levels were determined by western blotting and normalized to GAPDH. Two SDS gels were used for each experiment. Data represent means ± SEM from at least three independent experiments. $^{*}P<0.05$, $^{**}P<0.01$, $^{***}P<0.001$ compared to IFN-α2a treated cells.

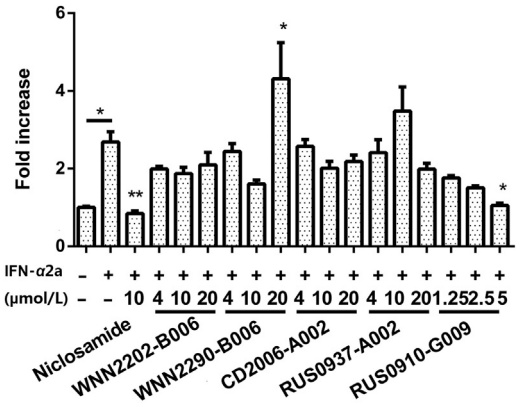

Figure 7 Effects of some confirmed hits on IRF7 transcription level in response to IFN-α2a treatment (1 h) in SH-SY5Y cells. Data represent mean expression fold ± SEM relative to GAPDH, measured from three independent experiments, each in triplicates. $^{*}P<0.05$, $^{**}P<0.01$, and $^{***}P<0.001$ compared to IFN-α2a treated cells.

IFN-α2a treatment for 1 h increased IRF7 mRNA transcription level by 2.09 ± 0.16 folds and 2.69 ± 0.26 folds compared to untreated controls for HEK (Supplementary Information Fig. S3) and SH-SY5Y (Fig. 7) cells, respectively. However, the treatment did not significantly affect IRF3 mRNA levels in both cell lines (1.25 ± 0.15 folds and 1.03 ± 0.04 folds for HEK and SH-SY5Y, respectively). Positive control niclosamide suppressed IRF7 level to a level close to normal (0.84 ± 0.07 folds) in SH-SY5Y cells.

Seven hits were tested in HEK-Blue IFNα/β cells (Fig. S3B) while 5 relatively non-toxic hits were investigated in SH-SY5Y cells (Fig. 7) in three concentrations (20, 10 and 4 μmol/L): they displayed variable inhibitory properties on IRF7 mRNA transcription but only RUS0910-G009 exhibited dose-dependency suppression.

4. Discussion

Type-I IFNs primarily activate the JAK-STAT signaling pathway. The normal function of the IFN system is essential to human health and disease interventions[28]. Numerous attempts to find inhibitors of type-I IFN signal transduction are based upon the clinical importance of this pathway covering tumor growth[29,30], viral infection, rheumatoid arthritis[10,17,31], systemic lupus erythematosus, Alzheimer's disease and neuroinflammatory diseases[8].

In this study, we utilized SEAP reporter gene assay in specially engineered HEK-Blue IFNα/β cells to detect JAK-STAT pathway activities induced by type-I IFN. This cell line is stably transfected with STAT2, IRF9, and SEAP genes. Following activation by type-I IFN, ISGF3 complex will bind to ISRE in the promoter of IFN-stimulated genes (ISG). SEAP, attached to ISG54 promoter, will be then be easily expressed and secreted to the culture medium and measured spectrophotometrically by detection reagent. It has been commonly used for measurement of type-I IFN activity from cell culture supernatant[32].

Application of ISRE to different screening systems has been reported previously, usually linked with a luciferase gene reporter[14–16]. In our case, cells were stimulated with recombinant human IFN-α2a, a key innate cytokine and essential to antiviral immune responses[33]. IFN-α2a was reported to robustly activate signaling pathways as fast as 5 min for TYK2 phosphorylation and 10 min for STAT phosphorylation at 30 ng/mL concentration[21]. We optimized the incubation time with QUANTI-Blue and the IFN concentration to enhance the signal readout. This validation process was successful as demonstrated by high quality assay parameters such as CV, *Z'* factor and *S/B* ratio. Thus, we have developed an HTS assay to search for novel inhibitors of IFN-α2a signaling. In the primary screening of 32,000 compounds, 457 initial hits (1.4%) were identified. Secondary screening and dose-response experiments resulted in 25 confirmed hits. Of which, 18 exhibited IC_{50} values below 10 μmol/L and 7 were capable of inhibiting phosphorylation of STAT1 Try701 and/or STAT3 Tyr705 at 20 μmol/L and two of them displayed consistent dose-dependent features. RUS0910-G009 appears most active in the two engineered cell lines used: it also caused notable IRF7 mRNA suppression.

In summary, by use of a SEAP reporter gene based HTS assay, we were able to discover 25 potential small molecule inhibitors of the IFN-α2a signaling pathway. Several of them were further characterized for cytotoxicity, inhibition on STAT phosphorylation and suppression of IRF7 transcription. It seems that this SEAP reporter gene assay is a viable approach to the discovery of small molecules interfering with type-I IFN action, especially *via* the JAK-STAT pathway. It provides an alternative to other screening systems such as thermofluor-[13] and fluorescence resonance energy transfer (FRET)-based[34] techniques.

Acknowledgments

We are indebted to Caihong Zhou, Ji Wu and Qiang Shen for technical assistance. This work was partially supported by grants from Shanghai Science and Technology Development Fund (to MWW: 15DZ2291600) and the Thousand Talents Program in China (to MWW: [2011]166). PJC was a recipient of an Australian Research Council Future Fellowship and CAS President's International Fellowship Initiative (PIFI). The funders had no role in study design, data collection and analysis, decision to publish, or manuscript preparation.

Appendix A. Supporting information

Supplementary data associated with this article can be found in the online version at https://doi.org/10.1016/j.apsb.2018.07.005.

References

1. McNab F, Mayer-Barber K, Sher A, Wack A, O' Garra A. Type I interferons in infectious disease. *Nat Rev Immunol* 2015;**15**:87–103.
2. Ng CT, Mendoza JL, Garcia KC, Oldstone MB. Alpha and beta type 1 interferon signaling: passage for diverse biologic outcomes. *Cell* 2018;**164**:349–52.
3. Jonasch E, Haluska FG. Interferon in oncological practice: review of interferon biology, clinical applications, and toxicities. *Oncologist* 2001;**6**:34–55.
4. Capobianchi MR, Uleri E, Caglioti C, Dolei A. Type I IFN family members: similarity, differences and interaction. *Cytokine Growth Factor Rev* 2015;**26**:103–11.
5. Oie S, Ono M, Yano H, Maruyama Y, Terada T, Yamada Y, et al. The up-regulation of type I interferon receptor gene plays a key role in hepatocellular carcinoma cells in the synergistic antiproliferative effect by 5-fluorouracil and interferon-α. *Int J Oncol* 2006;**29**:1469–78.

6. Mcglasson S, Jury A, Jackson A, Hunt D. Type I interferon dysregulation and neurological disease. *Nat Rev Neurol* 2015;**11**:515–23.
7. Bialas AR, Presumey J, Das A, van der Poel CE, Lapchak PH, Mesin L, et al. Microglia-dependent synapse loss in type I interferon-mediated lupus. *Nature* 2017;**546**:539–43.
8. Taylor JM, Moore Z, Minter MR, Crack PJ. Type-I interferon pathway in neuroinflammation and neurodegeneration: focus on Alzheimer's disease. *J Neural Transm* 2018;**125**:797–807.
9. Hervas-Stubbs S, Perez-Gracia JL, Rouzaut A, Sanmamed MF, Le Bon A, Melero I. Direct effects of type I interferons on cells of the immune system. *Clin Cancer Res* 2011;**17**:2619–27.
10. Cornez I, Yajnanarayana SP, Wolf AM, Wolf D. JAK/STAT disruption induces immune-deficiency: rationale for the development of JAK inhibitors as immunosuppressive drugs. *Mol Cell Endocrinol* 2017;**451**:88–96.
11. Kirou KA, Gkrouzman E. Anti-interferon alpha treatment in SLE. *Clin Immunol* 2013;**148**:303–12.
12. Chasset F, Arnaud L. Targeting interferons and their pathways in systemic lupus erythematosus. *Autoimmun Rev* 2018;**17**:44–52.
13. de Araujo ED, Manaswiyoungkul P, Israelian J, Park J, Yuen K, Farhangi S, et al. High-throughput thermofluor-based assays for inhibitor screening of STAT SH2 domains. *J Pharm Biomed Anal* 2017;**143**:159–67.
14. Patel DA, Patel AC, Nolan WC, Zhang Y, Holtzman MJ. High throughput screening for small molecule enhancers of the interferon signaling pathway to drive next-generation antiviral drug discovery. *PLoS One* 2012;**7**:e36594.
15. Tai ZF, Zhang GL, Wang F. Identification of small molecule activators of the Janus kinase/signal transducer and activator of transcription pathway using a cell-based screen. *Biol Pharm Bull* 2012;**35**:65–71.
16. Wonganan O, He Y, Shen X, Wongkrajang K, Suksamrarn A, Zhang G, et al. 6-Hydroxy-3-*O*-methyl-kaempferol 6-*O*-glucopyranoside potentiates the anti-proliferative effect of interferon *α/β* by promoting activation of the JAK/STAT signaling by inhibiting SOCS3 in hepatocellular carcinoma cells. *Toxicol Appl Pharmacol* 2017;**336**:31–9.
17. Schwartz DM, Kanno Y, Villarino A, Ward M, Gadina M, O'Shea JJ. JAK inhibition as a therapeutic strategy for immune and inflammatory diseases. *Nat Rev Drug Discov* 2017;**16**:843–62.
18. Taylor JM, Minter MR, Newman AG, Zhang M, Adlard PA, Crack PJ. Type-1 interferon signaling mediates neuro-inflammatory events in models of Alzheimer's disease. *Neurobiol Aging* 2014;**35**:1012–23.
19. Minter MR, Taylor JM, Crack PJ. The contribution of neuroinflammation to amyloid toxicity in Alzheimer's disease. *J Neurochem* 2016;**136**:457–74.
20. Jiao J, Kaur N, Lu B, Reeves SA, Halvorsen SW. Initiation and maintenance of CNTF-Jak/STAT signaling in neurons is blocked by protein tyrosine phosphatase inhibitors. *Mol Brain Res* 2003;**116**:135–46.
21. Dedoni S, Olianas MC, Onali P. Interferon-*β* induces apoptosis in human SH-SY5Y neuroblastoma cells through activation of JAK-STAT signaling and down-regulation of PI3K/Akt pathway. *J Neurochem* 2010;**115**:1421–33.
22. Ren X, Duan L, He Q, Zhang Z, Zhou Y, Wu D, et al. Identification of niclosamide as a new small-molecule inhibitor of the STAT3 signaling pathway. *ACS Med Chem Lett* 2010;**1**:454–9.
23. Zhang J-H, Chung TDY, Oldenburg KR. A simple statistical parameter for use in evaluation and validation of high throughput screening assays. *J Biomol Screen* 1999;**4**:67–73.
24. Main BS, Zhang M, Brody KM, Ayton S, Frugier T, Steer D, et al. Type-1 interferons contribute to the neuroinflammatory response and disease progression of the MPTP mouse model of Parkinson's disease. *Glia* 2016;**64**:1590–604.
25. Minter MR, Zhang M, Ates RC, Taylor JM, Crack PJ. Type-1 interferons contribute to oxygen glucose deprivation induced neuroinflammation in BE(2) M17 human neuroblastoma cells. *J Neuroinflamm* 2014;**11**:43.
26. Paul F, Pellegrini S, Uzé G. IFNA2: the prototypic human alpha interferon. *Gene* 2015;**567**:132–7.
27. Molle C, Goldman M, Goriely S. Critical role of the IFN-stimulated gene factor 3 complex in TLR-mediated IL-27p28 gene expression revealing a two-step activation process. *J Immunol* 2010;**184**:1784–92.
28. Arimoto K, Löchte S, Stoner SA, Burkart C, Zhang Y, Miyauchi S, et al. STAT2 is an essential adaptor in USP18-mediated suppression of type I interferon signaling. *Nat Struct Mol Biol* 2017;**24**:279–89.
29. Chau MN, Banerjee PP. Development of a STAT3 reporter prostate cancer cell line for high throughput screening of STAT3 activators and inhibitors. *Biochem Biophys Res Commun* 2008;**377**:627–31.
30. Page BDG, Ball DP, Gunning PT. Signal transducer and activator of transcription 3 inhibitors: a patent review. *Expert Opin Ther Pat* 2011;**21**:65–83.
31. Thoma G, Drückes P, Zerwes H-G. Selective inhibitors of the Janus kinase Jak3—Are they effective?. *Bioorg Med Chem Lett* 2014;**24**:4617–21.
32. Dallari S, Macal M, Loureiro ME, Jo Y, Swanson L, Hesser C, et al. Src family kinases Fyn and Lyn are constitutively activated and mediate plasmacytoid dendritic cell responses. *Nat Commun* 2017;**8**:14830.
33. Horvath CM. The Jak-STAT pathway stimulated by interferon *α* or interferon *β*. *Sci STKE* 2004;**2004**:tr10.
34. Robers MB, Horton RA, Bercher MR, Vogel KW, Machleidt T. High-throughput cellular assays for regulated posttranslational modifications. *Anal Biochem* 2008;**372**:189–97.